Variability of Updraft and Downdraft Characteristics in a Large Parameter Space Study of Convective Storms

CODY KIRKPATRICK

University of Alabama in Huntsville, Huntsville, Alabama

EUGENE W. MCCAUL JR. AND CHARLES COHEN

Universities Space Research Association, Huntsville, Alabama

(Manuscript received 27 June 2008, in final form 16 October 2008)

ABSTRACT

Over 200 convective storm simulations are analyzed to examine the variability in storm vertical velocity and updraft area characteristics as a function of basic environmental parameters. While it is known that bulk properties of the troposphere such as convective available potential energy (CAPE) and deep-layer wind shear exert significant influence over updraft intensity and area, additional parameters such as the temperature at the cloud base, the height of the level of free convection (LFC), and the vertical distribution of buoyancy also have an effect. For example, at low CAPE, updraft strength is strongly related to the vertical distribution of buoyancy, and also to the bulk environmental wind shear. More generally, updraft area and its temporal variability both tend to increase in environments where the LFC is raised. Additionally, in environments with persistent storms, downdraft strength is sensitive to the bulk shear, environmental temperature, and LFC height. Using multiple linear regression methods, the best combinations of environmental parameters explain up to 81% of the interexperiment variance in second-hour mean peak updraft velocity, 74% for midlevel updraft area, and 64% for downdraft velocity. Downdraft variability is explained even less well (49%) when only persistent storms are considered. These idealized simulation results show that it is easier to predict storm updraft characteristics than those of the downdraft.

1. Introduction

Knowledge of the environmental conditions that affect the intensity of deep, moist convection is critical to weather forecasters, researchers, and the public. Under the right conditions, air parcels that are lifted to the level of free convection (LFC) by some external forcing mechanism will continue to rise and exploit the convective available potential energy (CAPE) present, accelerating vertically upward. Pure parcel theory (e.g., Dutton 1976) suggests that the peak vertical velocity of an updraft is related to CAPE by $w_{max} = (2\text{CAPE})^{0.5}$. However, this serves only as a theoretical estimate, and not an exact forecast of updraft intensity, primarily because of mass loading due to condensate, entrainment of ambient air into the updraft, and the action of pressure perturbation effects.

Prior numerical modeling studies have revealed that, in addition to CAPE, other bulk parameters such as deep tropospheric wind shear are important regulators of overall storm evolution (Weisman and Klemp 1982, 1984). More recent studies have shown that additional environmental properties are important, such as the vertical distribution of buoyancy (McCaul and Weisman 2001), and the mixed layer and moist layer depths (McCaul and Cohen 2002). Updraft strength and precipitation efficiency, among other storm properties, can also be affected by environmental temperature (McCaul et al. 2005, hereafter MCK05) and the characteristics of the microphysical parameterizations employed (Cohen and McCaul 2006). Adlerman and Droegemeier (2005) clarified the importance of environmental vertical wind shear, finding that ''the strongest [mesocyclones] occur when the largest shears are confined to the shallowest depths.'' Many of these studies, however, focused on the

Corresponding author address: Cody Kirkpatrick, University of Alabama in Huntsville, 320 Sparkman Dr., Room 3078, Huntsville, AL 35899.
E-mail: cody.kirkpatrick@uah.edu

DOI: 10.1175/2008MWR2703.1

relationship between environmental conditions and the storm updraft. In this work we also consider the effects of these parameters on the downdraft. Downdraft outflows can help promote tornadogenesis (e.g., Lemon and Doswell 1979; Fujita 1981), maintain existing convection (e.g., Rotunno et al. 1988; Weisman 1993), trigger new convection (e.g., Droegemeier and Wilhelmson 1985), and generally influence storm motion and structure (e.g., Knupp 1987, 1988; Wakimoto 2001). Knowledge of downdraft intensity is useful in forecasting damaging winds and hazardous wind shear.

Beyond the numerical studies mentioned above, numerous observational studies have worked to identify environmental conditions that can influence deep moist convection. Early studies (e.g., Byers and Braham 1949; Fawbush and Miller 1954; Beebe 1955; Marwitz 1972) described the general kinematic and thermodynamic conditions favorable for strong storms and tornadoes. More recently, Rasmussen and Straka (1998) studied the effect of upper-level winds on the storm precipitation distribution, which can affect intensity and organization of the low-level updraft. Rasmussen and Blanchard (1998) associated reports of tornadoes, hail, damaging wind, and clusters of cloud-to-ground lightning strikes with nearby soundings to establish the mean conditions for each weather type. Environmental parameters such as the LCL and mean shear in some layer (Rasmussen and Blanchard used 0–4 km) show some stratification for soundings associated with ordinary convection, supercells, and tornadoes. Analysis of many years of soundings (Brooks and Craven 2002) has yielded additional information, suggesting that low LCLs collocated with increased low-level shear (e.g., 0–1 km) enhance tornado likelihood, with different configurations that enhance the potential for strong wind gusts or large hail. Some atmospheric variables are able to discriminate between storms that produce strong or violent tornadoes (e.g., F2 or greater) and those that do not produce tornadoes at all (Thompson et al. 2003). Studies have also attempted to describe the potential for damaging wind gusts or large hail in terms of environmental conditions (e.g., Evans and Doswell 2001; Kuchera and Parker 2006).

MCK05 describe the nomenclature of the Convection Morphology Parameter Space Study (COMPASS), a large set of simulations of discrete convective storms. The base set of 216 COMPASS simulations, each initiated with a unique idealized environmental profile (within a seven-dimensional subset of an eight-dimensional parameter space), is the foundation of this work. In this article we describe some of the trends seen in our simulated storms, focusing on the updrafts and downdrafts. We treat our simulated storms as if they are an ''observational'' dataset for statistical purposes, so that we can associate particular storm evolutions with background environmental conditions. This approach has been followed in certain previous COMPASS studies (Kirkpatrick et al. 2006, 2007). We note that the envelope of conditions considered in our simulations (see Table 1) spans a wide range of atmospheric environments, and is not exclusive of any particular storm type (supercells, ordinary cells, etc.). All COMPASS environments are designed to be horizontally homogeneous and time invariant during the simulations.

Section 2 describes the COMPASS simulation set and analysis methods. The environmental conditions that promote strong, large updrafts and downdrafts, as well as the conditions that encourage variability in draft size and strength, are explored in section 3. Our research also examines the use of reversible CAPE (RCAPE) versus pseudoadiabatic CAPE (PCAPE) in anticipating updraft strength; these findings are presented in section 4. The present study differs from that reported in previous research (McCaul and Weisman 2001; McCaul and Cohen 2002; MCK05) in that we consider bulk variations in storm updraft and downdraft strength across the entire available parameter space, instead of those associated with changing only one or two environmental parameters.

2. Data and methodology

The COMPASS simulations are performed using a modified version of the Regional Atmospheric Modeling System (RAMS; Pielke et al. 1992), version 3b, with modifications as described in MCK05. RAMS is a nonhydrostatic cloud model that solves the fully compressible equations of motion (Tripoli and Cotton 1982) using a time-splitting scheme (Klemp and Wilhelmson 1978). The model includes prognostic equations for six species of hydrometeors (rain, hail, graupel, pristine ice, snow, and aggregates) and a diagnostic equation for the cloud water–mixing ratio. Microphysical parameters that define the size distributions of the various particle species are held fixed to simplify interpretation of the simulation results. Some additional characteristics of the model are described in Kirkpatrick et al. (2007, their Table 4).

Eight environmental variables define the parameter space (Table 1). These eight parameters completely determine our idealized initial profiles (see also MCK05; Kirkpatrick et al. 2007). CAPE takes on one of three values. The hodographs employed are approximately semicircles (of varying radius) through the depth of the domain. The CAPE and shear are also governed by shape parameters that define the vertical distribution of

TABLE 1. Environmental parameters used to construct the profiles in this study.

Parameter	Abbreviation	Values
Bulk pseudoadiabatic CAPE	PCAPE	800, 2000, 3200 J kg^{-1}
Hodograph radius	VMAG	8, 12, 16 m s^{-1}
Level of max buoyancy	ZMAXB	Two values per CAPE
Level of max v wind	ZMAXV	Two values per CAPE
LCL	LCL	0.5 or 1.6 km
LFC	LFC	0.5 or 1.6 km
Atmospheric PW, implemented as LCL temperature	T_{LCL}	15.5° and 23.5° for LCL = 0.5 km
Relative humidity everywhere above the LFC		Fixed at 90%

the quantity. In our simulations, there are two cases for the buoyancy and shear profile parameters: a ''concentrated'' and a ''distributed'' case. The distributed profile is one in which the variable (shear or buoyancy) is spread over a deeper layer with a maximum in the midtroposphere; in the concentrated profile, the level of the variable maximum is in the lower troposphere. Furthermore, distributed shear profiles have a smaller magnitude of low-level shear when compared to the concentrated shear profiles (Table 2). In this study, the eighth parameter, relative humidity in the free troposphere (i.e., everywhere above the LFC) is fixed at 90%. As a result of all the other parameters combined [3 values for CAPE, 3 hodograph radius magnitudes, 2 wind profile shapes and 2 buoyancy profile shapes per CAPE, 3 configurations of lifting condensation level (LCL) and LFC, and a high or low value of temperature at the cloud base], 216 simulations are explored.

Each simulation is initialized with a moist, LCL-conserving thermal bubble in an otherwise horizontally homogeneous domain. The model is configured with 500-m horizontal grid spacing and a vertical mesh that is stretched, from 250-m spacing near the surface to 750 m at 20 km. A wave-absorbing layer is specified from 20 km up to the top (24.5 km). The Coriolis acceleration is neglected. Model output is saved every 5 min during the 2-h simulations. Storms are tracked by identifying the location of the maximum updraft velocity at a model level approximately 2 km above the LFC. The dominant right-moving storm in each simulation (if present) is tracked,[1] and values of different storm properties from each output time in the second hour are averaged to provide a storm's overall statistics. We define a storm as ''persistent'' if it exists for the entire 2-h simulation. There are rare cases where the left-moving storm in a simulation temporarily has a stronger updraft than the right-mover; study of the left-moving storms in our database is an area of continued research.

[1] If the storm being tracked undergoes a split, we follow the right member of the split.

Using the seven environmental parameters that are variable, stepwise regression is performed against certain storm properties. Since only two or three values of each parameter are available, all regressions are of the linear form. In this paper, results for mean second-hour updraft velocity (WMAX; m s^{-1}), area (at 5 km; WAREA5; km^2), and downdraft velocity (WMIN; m s^{-1}) are presented. The variance of the 13 values averaged from the second hour (60–120 min, in 5-min intervals) of a simulation can be used as a measure of temporal variability for any particular storm property; these variances will also be discussed.

3. Results and discussion

a. *WMAX*

The distribution of second-hour updraft velocities as a function of PCAPE and bulk shear (hodograph radius; VMAG) is shown in Fig. 1a. The distribution is similar to those found in previous parameter space studies (e.g., Weisman and Klemp 1982, 1984), with the strongest updrafts occurring when both PCAPE and shear are large. Storms are much weaker when either PCAPE or VMAG are small, and are especially weak when both are small. Also evident are some of the complexities of relating WMAX to environmental parameters. Simulations with a raised LFC feature generally stronger updrafts for all nine bulk CAPE–VMAG combinations, but with greater temporal variability for six of nine bulk

TABLE 2. The 0–6-km shear magnitudes (m s^{-1}) for all possible choices of VMAG and ZMAXV. The 0–1-km shear magnitude is given in parentheses.

	VMAG (m s^{-1})		
ZMAXV (km)	8	12	16
9.3	9 (2)	14 (3)	19 (5)
7.7	11 (3)	16 (4)	21 (6)
6.0	12 (4)	18 (5)	24 (7)
4.4	14 (5)	21 (7)	28 (10)
2.7	16 (8)	24 (12)	32 (16)

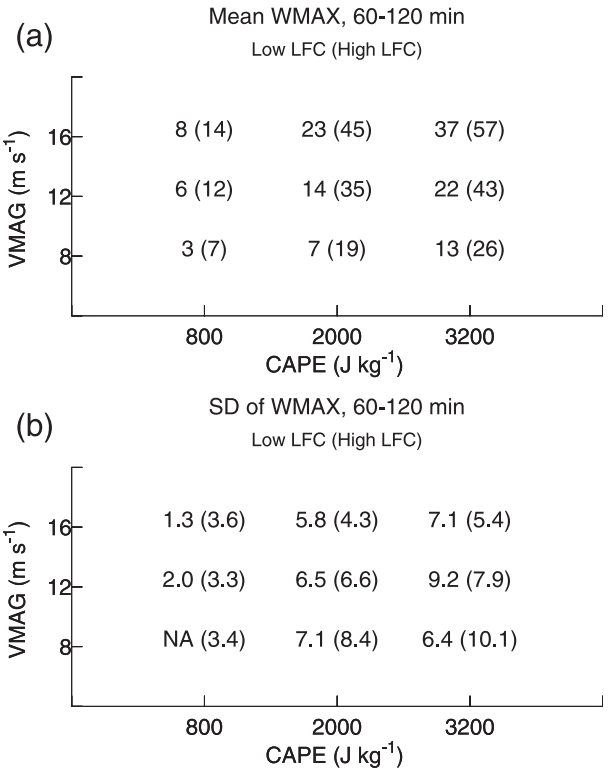

FIG. 1. (a) Second-hour mean WMAX (m s^{-1}) as a function of CAPE and VMAG for all 216 simulations, with further stratification into low (high) LFC simulations. Each low (high) LFC bin consists of 8 (16) simulations. (b) As in (a), but showing the average second-hour temporal std devs of WMAX (m s^{-1}) for the subset of 139 persistent storms. There are no persistent storms in the "NA" category.

CAPE–VMAG combinations (Fig. 1b). Not surprisingly, the single environmental parameter that correlates best with WMAX is CAPE (solid line, Fig. 2). CAPE is actually represented here as $(2\ \mathrm{PCAPE})^{0.5}$, to provide a variable with the same units as WMAX. The initial linear correlation ($r^2 = 0.32$, for WMAX versus $(2\ \mathrm{PCAPE})^{0.5}$; Table 3) is lower than one might expect. However, this does not diminish the fact that PCAPE appears to be the most important parameter when attempting to explain WMAX. When a two-parameter combination is considered, PCAPE and hodograph radius ("VMAG" in Fig. 2 and Table 3) provide the best correlation to WMAX. The hodograph radius (VMAG) is effectively an expression of the bulk tropospheric shear, and sufficient amounts of both bulk shear and CAPE must be present for strong, persistent convection to occur.

A third environmental condition that contributes to updraft intensity is the temperature at cloud base (T_{LCL}), roughly related to atmospheric precipitable water (PW; MCK05). All other parameters held equal, when the environment is cooler, there is a greater contribution to buoyancy from the latent heat of fusion at low altitudes, less water vapor overall, and less dominance of the collision–coalescence precipitation process. Thus, water mass in the updraft is reduced and updrafts tend to be stronger. A fourth parameter is the height of the LFC. When the LFC is raised within reasonable bounds, a deeper layer of moist inflow air is accessible to the updraft, increasing updraft overturning efficiency and producing generally wider and stronger updrafts (McCaul and Cohen 2002).

The addition of a fifth parameter, the altitude of maximum buoyancy (ZMAXB), to the WMAX regression further improves the results ($r^2 = 0.73$). The vertical distribution of the CAPE present has been shown to be an important modulator of updraft intensity (e.g., McCaul and Weisman 1996, 2001; Wicker and Cantrell 1996). High concentrations of buoyancy near the LFC can help updrafts overcome strong shear, and the effects of buoyancy concentration appear to be most significant in CAPE-starved regimes: in fact, for 800-CAPE simulations only, the correlation coefficient between ZMAXB and WMAX is much larger than for 2000- and 3200-CAPE simulations ($r = -0.65$ versus -0.20 versus -0.19).

With these five parameters, nearly three-fourths (73%) of the interexperiment variance in WMAX can be explained. A multiple linear regression using these parameters produces a mean absolute error (MAE) of 7.6 m s^{-1} if the 16 predictions of WMAX less than 0 m s^{-1} (which are unphysical) are truncated as zeros. If the entire set of seven parameters is used, 81% of the interexperiment variance can be explained, and the MAE decreases to 5.9 m s^{-1} (again, if unphysical values are truncated to zero). These regression and correlation results are illustrated by the solid curve in Fig. 2. The regression coefficients are shown in Table 3, and WMAX predictions (when $n = 7$) are compared against the simulated WMAX values in Fig. 3. Note that there are a few substantial outliers in Fig. 3a. In particular, the regression predicted that five environments would produce updrafts of about 15 m s^{-1} or greater (cluster of circles along the abscissa in Fig. 3c), and these simulations did not produce sustained convection. These environments merit special discussion.

The five environments in which the linear regression incorrectly predicts a strong updraft, while none occurs in the simulation, are all characterized by 800-CAPE, a large (VMAG = 16 m s^{-1}) hodograph radius, distributed buoyancy, and concentrated shear. This is a "CAPE-starved" environment that is hostile to convective storms, since weak updraft impulses are unlikely to remain sufficiently upright in such weakly buoyant yet strongly sheared conditions. For the 12 simulations

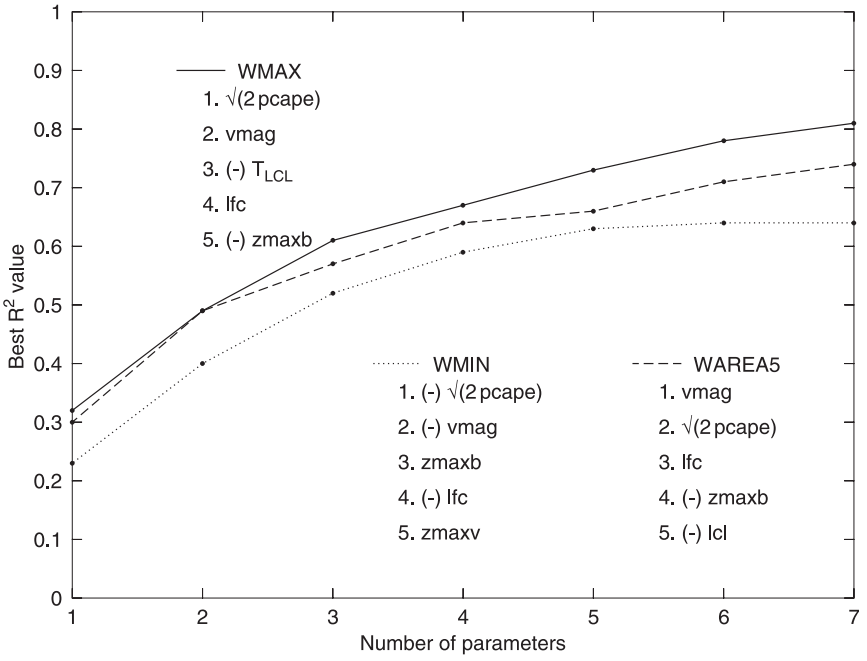

FIG. 2. Best multiple linear regressions of WMAX and WMIN (m s^{-1}) and WAREA5 (km^2) as a function of the number of parameters used. The first five parameters for each storm property are listed in order of importance. Parameters with a negative regression coefficient are noted by "(-)." Each dot represents a new linear equation; for WMAX (WAREA5), the coefficients are given in Table 2 (Table 3).

with 800-CAPE, a 16 m s^{-1} hodograph, and distributed (concentrated) buoyancy, the mean second-hour updraft intensity is 3 m s^{-1} (22 m s^{-1}). CAPE-starved storms generally become more intense if the low-level lapse rates in their environments are increased (McCaul and Weisman 2001). The failure of the linear regression technique for these cases likely occurs because high shear environments are supportive of strong updrafts, but only when CAPE or low-level buoyancy is sufficient. There is apparently a rather sharp cutoff in the parameter space, which separates sustained from unsustained convection, and this cutoff is not well handled by standard linear regression techniques. Four of these five failure environments also feature a high LFC, which supports large, strong storms, but only if other conditions are also favorable.

Figure 1b shows the temporal variability of WMAX in the CAPE–VMAG parameter space. The variability is studied only for the 139 simulations that produced a sustained storm through the entire 2 h of the simulation. Updraft intensities are more variable over a storm's life cycle when the CAPE is larger and/or when VMAG is weaker. At low CAPE and/or low VMAG, updrafts are slightly more variable when the LFC is raised (standard

TABLE 3. Regression coefficients (b_n) and variances (r^2) for each of the stepwise regression equations for WMAX depicted in Fig. 2. The parameters are listed by their order of inclusion in the equation. The number of parameters in the equation is given as n. As an example, the equation when the one-parameter equation is used would be $w_{\text{predicted}} = 0.677 \times (2\ \text{PCAPE})^{0.5} - 17.286$.

		$b_0 \ldots b_n$						
n	(y intercept)	−17.286	−46.473	−21.339	−38.539	−35.609	−22.800	−20.557
1	√(2PCAPE) (m s^{-1})	0.677	0.677	0.677	0.677	0.903	0.903	1.077
2	VMAG (m s^{-1})		2.432	2.432	2.432	2.432	2.432	2.432
3	T_{LCL} (°C)			−1.411	−1.138	−1.138	−1.623	−1.623
4	LFC (km)				10.005	10.005	14.457	14.457
5	ZMAXB (km)					−2.789	−2.789	−2.777
6	LCL (km)						−11.131	−11.131
7	ZMAXV (km)							−2.147
	r^2	0.32	0.49	0.61	0.67	0.73	0.78	0.81

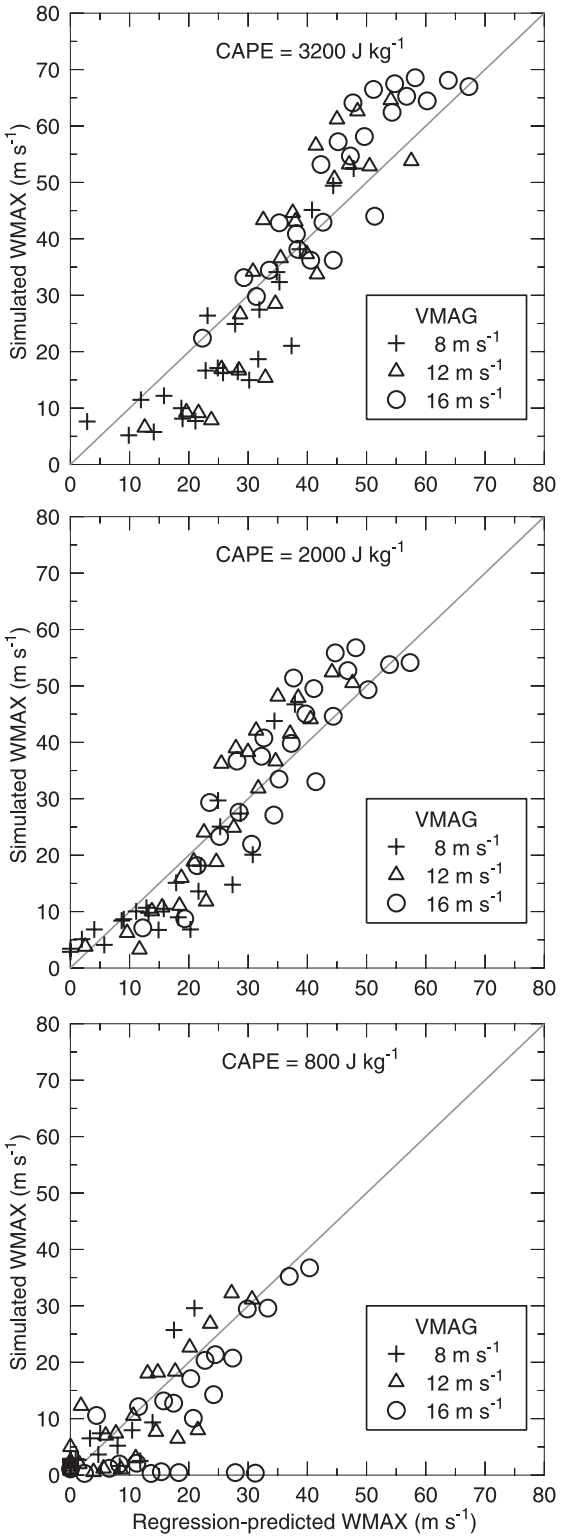

FIG. 3. Comparison of simulated WMAX to the value predicted by a seven-parameter linear regression for all simulations. Any predicted value of WMAX less than 0 m s^{-1} has been graphed as 0. Panels are CAPE bins, with values (J kg^{-1}) shown. The different symbols represent values of VMAG (m s^{-1}).

deviations increase 1–1.5 m s^{-1}), but vary less as the LFC is raised when both CAPE and VMAG are large.

Based on a subjective assessment of simulation output, more convective cells are produced when CAPE is large, and especially when ZMAXB is low (low-level lapse rates are increased). Since our simulations are initiated with a single thermal bubble, these environments may be prone to more multicell convection, generation of updrafts by forcing along density gradients, etc. Quantification of storm cell characteristics in the dataset is an area of continued research.

b. *WAREA5*

Updraft area[2] (WAREA5) behavior is also dominated by VMAG and CAPE (Fig. 4). Generally speaking, strong updrafts are also large ($r^2 = 0.76$ for WMAX versus WAREA5 in the simulation set), and the regressions show how WAREA5 depends on VMAG, CAPE, and the other environmental parameters (Table 4). Updraft area is also increased when the LFC is raised (third parameter added in Fig. 2 and Table 4), which reduces the likelihood that the updraft will ingest reduced-θ_e air that resides above the moist layer (McCaul and Cohen 2002). At high LFC, WAREA5 sensitivity to CAPE is almost nonexistent for CAPE $\geq$ 2000 J kg^{-1} (Fig. 4). The raised LFC is also critical to the vertical development of storms at 800-CAPE. Wider updrafts also deviate farther away from the mean wind, as observed by Newton and Fankhauser (1975) and shown analytically by Davies-Jones (2002). Indeed, in the simulation set used herein, storms with a 1.6-km LFC deviate farther from the mean wind than storms with a 0.5 km LFC (Kirkpatrick et al. 2007). These three parameters (CAPE, VMAG, and LFC) are the primary controls of updraft area in our simulations (see Fig. 5).

The levels of maximum buoyancy (ZMAXB) and v wind (ZMAXV) exhibit secondary control on updraft area, since they strongly contribute to low-level storm organization (Table 4). When buoyancy and shear are concentrated at low altitudes, updraft area and intensity are enhanced (McCaul and Weisman 2001). These effects are a function of other aspects of the environment, however. For example, steep low-level lapse rates (lower ZMAXB) exhibit much the same CAPE-dependent relationship to WAREA5 as to WMAX, correlating best at 800-CAPE and poorly for 2000- and 3200-CAPE sets (−0.50 versus −0.18 versus 0.18). Conversely, at 800-CAPE, increasing the low-level shear can lead to storms that do not persist beyond the initial thermal impulse; those that do survive are usually narrow and shallow.

[2] The area of the updraft with intensity of at least 2 m s^{-1}.

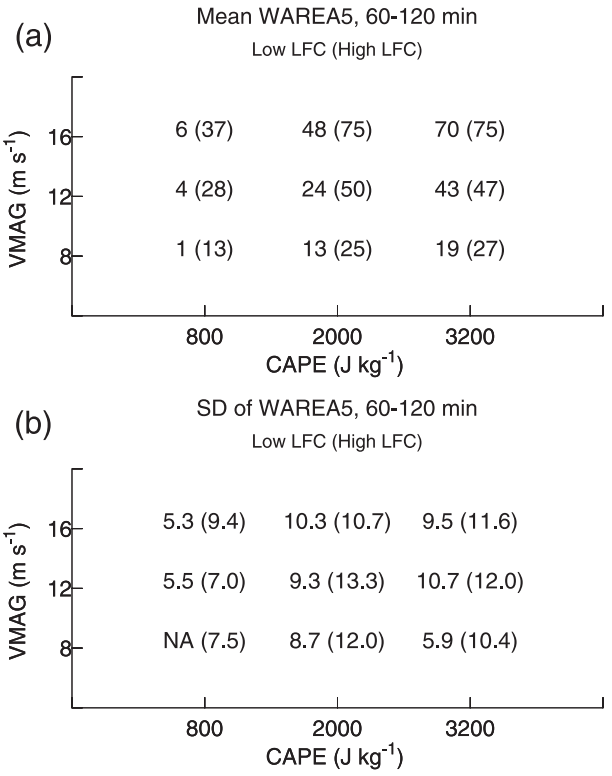

FIG. 4. As in Fig. 1, but for WAREA5 (km^2).

Temporal variability in WAREA5 increases primarily when low-level lapse rates are minimized (i.e., the buoyancy is distributed through deep layers and ZMAXB is large; Table 5). This is related to an increase in the pulselike nature of storms in distributed buoyancy environments. High LFC and large PCAPE also lead to increased temporal variability of WAREA5. The variability is decreased when T_{LCL} (i.e., PW) is raised, possibly because storms in higher-T_{LCL} environments tend to be weaker (Table 3) and smaller (Table 4). The *relative* variability of WAREA5 (not shown) is greatest when CAPE is low and VMAG is small, where updrafts are narrower to begin with. Updraft areas in those environments vary by an average of 40% over their lifetimes. At high CAPE and large VMAG, updraft areas generally vary by only about 20% during the second hour of the simulations.

c. *WMIN*

The stepwise regression of WMIN and environmental parameters is shown in Fig. 2 for all 216 simulations. These results suggest that WMIN is affected by largely the same parameters as WMAX. However, this is misleading, since the results from Fig. 2 will be contaminated by the 77 simulations that did not produce a persistent storm (and thus no downdraft). Including those results masks the conditions that are truly important for describing downdraft strength and maintenance in persistent storms. Thus, to examine environmental effects on the downdraft, we consider only the 139 simulations that produced a storm for the entire 2-h simulation (Table 6). For the present inquiry, this likely presents a more meaningful representation of the relationship between WMIN and the environment.

When only the persistent storms are considered, the strength of the downdraft is the most difficult storm property to parameterize in terms of the prestorm environmental conditions (using all seven parameters, $r^2 = 0.49$; Table 6). The most important parameters for predicting downdraft intensity are VMAG and T_{LCL}. As VMAG increases, storm organization typically increases, and the resulting stronger updrafts are usually accompanied by stronger downdrafts. Warmer cloud-base temperatures also give rise to stronger downdrafts, since a warmer environment will have a deeper layer below the melting level. This allows for more falling rain to evaporate than in our cold sounding cases. We note, however, that the complicated microphysical processes that occur in the downdraft can exert significant influence on its strength and depth (e.g., Wakimoto 2001). Phase changes of any liquid or solid condensate present can produce substantial latent heating or cooling in the

TABLE 4. As in Table 2, but for WAREA5 (km^2).

		$b_0 \ldots b_n$						
n	(y intercept)	−19.945	−66.219	−85.064	−80.406	−77.522	−62.001	−42.664
1	VMAG (m s^{-1})	4.690	4.690	4.690	4.690	4.690	4.690	4.690
2	√(2PCAPE) (m s^{-1})		0.758	0.758	1.118	1.341	1.341	1.341
3	LFC (km)			15.279	15.279	15.279	13.554	20.274
4	ZMAXB (km)				−4.433	−4.418	−4.418	−4.418
5	ZMAXV (km)					−2.760	−2.760	−2.760
6	T_{LCL} (°C)						−0.752	−1.485
7	LCL (km)							−16.805
	r^2	0.30	0.49	0.57	0.64	0.66	0.71	0.74

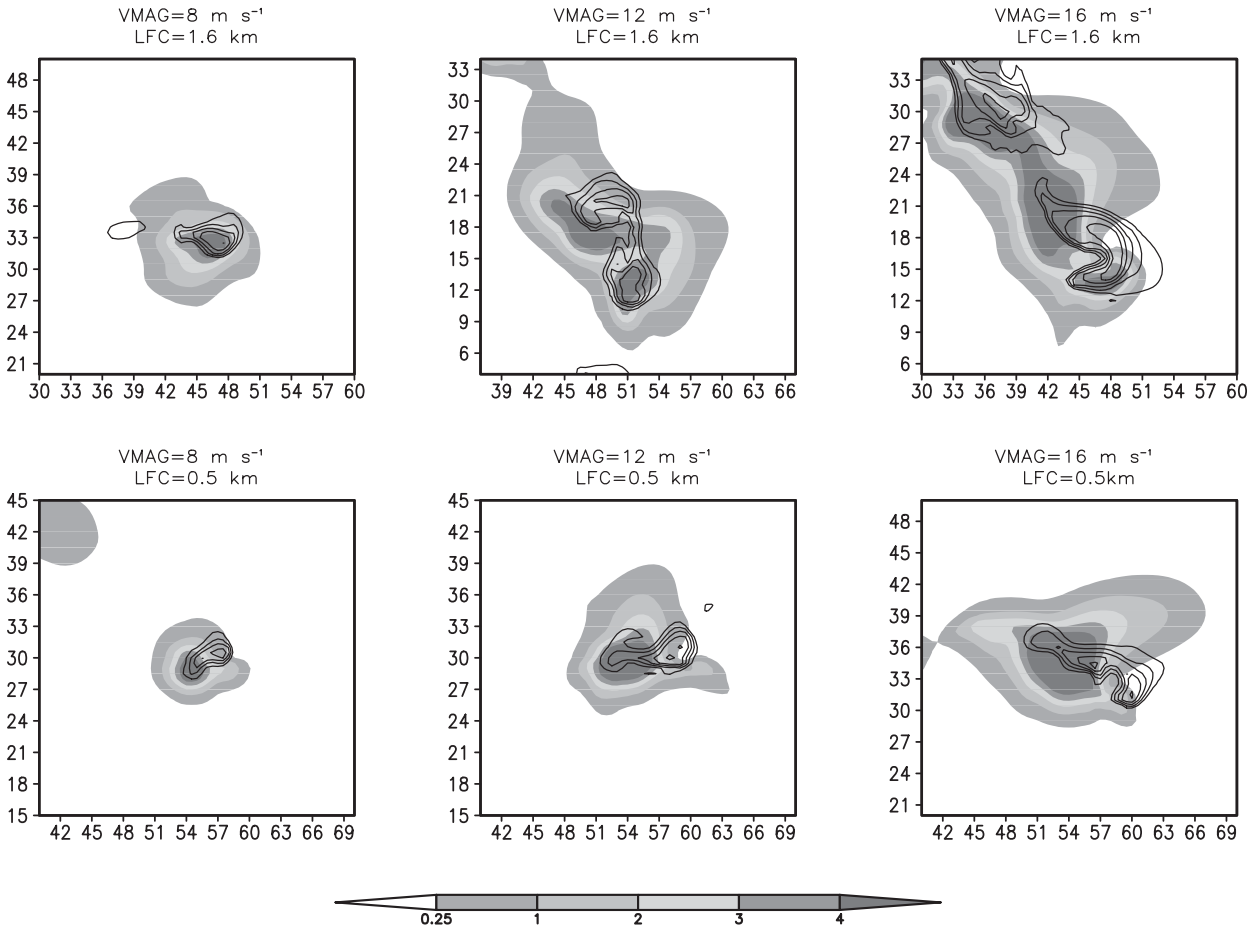

FIG. 5. Map of simulated updraft velocity at 5 km (contoured at 5 m s^{-1} intervals), and near-surface rainwater mixing ratio (shaded; g kg^{-1}) at 120 min for six simulated right-moving storms with varied hodograph radius and LFC. All simulations have CAPE = 2000 J kg^{-1}, concentrated buoyancy and shear, LCL = 0.5 km, and PW = 30 mm. Axes (km).

downdraft (e.g., Srivastava 1987). In our simulations, at low CAPE a large PW restrains both updraft and downdraft strength. However, at moderate and high CAPE, increasing PW results in greater production and fallout of precipitation, thus generating greater negative buoyancy (see MCK05). Even with the low overall correlation coefficient, the MAE for the seven parameter regression of WMIN is only 1.8 m s^{-1}. This is considerably less than the MAE for WMAX, but it must be remembered that here we do not consider ''null'' case environments, and the modeled downdrafts are somewhat weaker than the updrafts.

The warm environments noted above also lead to greater temporal variability of downdraft strength (Table 5), with T_{LCL} being the only environmental parameter that relates substantially to the temporal variability of WMIN. Evidently, the greater precipitation fallout and attendant increases in negative buoyancy work to multiply the nonlinear effects encountered in the downdraft. We also note that for some of the simulations herein, rain is falling into the storm outflow region, not into undisturbed air. Because the cold outflow is drier in the warmer sounding, even more evaporation can result (MCK05).

TABLE 5. Correlation coefficients of environmental parameters and storm temporal variability properties. The std dev over all 5-min values in the second hour is denoted by σ (thus, σ_{WMAX} is the std dev of all second-hour values of WMAX). Only the 139 cases with a persistent storm are included.

	σ_{WMAX}	σ_{WMIN}	σ_{WAREA5}
PCAPE	0.45	0.19	0.21
VMAG	−0.40	0.13	−0.01
ZMAXB	0.48	0.11	0.35
ZMAXV	0.21	0.05	0.16
LCL	0.05	0.07	0.08
LFC	0.02	0.15	0.26
T_{LCL}	−0.04	0.53	−0.20

TABLE 6. As in Table 2, but for WMIN (prediction in m s^{-1}), using only the 139 simulations that produced persistent convection through the entire 2-h simulation.

		$b_0 \ldots b_n$						
n	(y intercept)	−4.192	−1.379	1.912	6.206	6.589	7.345	7.828
1	VMAG (m s^{-1})	−0.377	−0.343	−0.366	−0.406	−0.443	−0.468	−0.459
2	T_{LCL} (°C)		−0.192	−0.220	−2.160	−0.211	−0.193	−0.221
3	LFC (km)			−1.921	−2.016	−2.127	−2.210	−2.003
4	√(2PCAPE) (m s^{-1})				−0.056	−0.106	−0.160	−0.157
5	ZMAXV (km)					0.544	0.476	0.551
6	ZMAXB (km)						0.468	0.462
7	LCL (km)							−0.511
	r^2	0.14	0.22	0.30	0.36	0.44	0.49	0.49

Gilmore and Wicker (1998) hypothesized that CAPE (in our case, PCAPE) may better relate to the updraft than a downdraft CAPE (DCAPE) relates to the downdraft.[3] For our 216 simulations, we find that to be true: $r^2 = 0.32$ for PCAPE versus WMAX, while $r^2 = 0.27$ for DCAPE versus WMIN. DCAPE by itself also relates better to WMIN than does PCAPE ($r^2 =$ 0.27 to 0.21). Figure 2 suggests that using PCAPE and VMAG together produces a better r^2 for WMIN (0.39), but using DCAPE and VMAG further improves the relationship ($r^2 = 0.44$). The implications of the difficulty in anticipating downdraft intensity are numerous: much of the ''sensible weather'' we observe is driven by the downdraft (e.g., precipitation intensity, cold pool size and intensity, and microbursts).

4. Reversible CAPE versus pseudoadiabatic CAPE

There are numerous ways to define CAPE (e.g., Emanuel 1994). PCAPE, used in this research and the foundation of parcel theory, assumes that all condensate is immediately removed from an air parcel upon formation. This is unrealistic, however, because observations show that at least some water mass is retained in updrafts. An RCAPE can also be defined, such that the negative buoyancy effects of condensate loading are accounted for. However, most formulations of RCAPE are unsatisfactory because they predict that condensate loading reaches a maximum at the updraft summit and do not account for precipitation fallout, again inconsistent with observations and simulations of convection. Actual amounts of condensate loading lie ''somewhere between the zero loading assumed by PCAPE and the significant loading assumed by RCAPE'' (MCK05).

MCK05, in a study of the effects of temperature on convective storms, presented evidence to suggest that RCAPE may provide a more accurate prediction of updraft strength than PCAPE. In their study (which used a subset of the 216 simulations considered herein), they found a consistent trend toward weaker updraft speeds when atmospheric temperature and PW are increased, all other parameters (including PCAPE) held equal. RCAPE, of course, is substantially reduced (consistent with the intensity of the simulated updraft) in high-PW environments. When expanding the MCK05 results to our set of 216 simulations, we find that, in fact, RCAPE provides a better estimate of mean second-hour WMAX than PCAPE in 215 (99.5%) of the simulations.[4] As a single variable in a linear correlation, RCAPE correlates better with WMAX than does PCAPE ($r^2 = 0.40$ to 0.32). These findings appear to support and strengthen the hypothesis of MCK05. We note, however, that RCAPE underpredicts the peak *instantaneous* WMAX in 33 of 216 simulations, thus illustrating the difficulties with using RCAPE exclusively in convective forecasting. Interestingly, the full seven-parameter regression using RCAPE is a *poorer* predictor of WMAX than when PCAPE is used (r^2=0.74 versus 0.81). RCAPE's implicit inclusion of T_{LCL} effects (e.g., T_{LCL} is the least important parameter in Table 7) may explain why its regression performs better initially.

5. Conclusions

The bulk statistics of a large set of simulated convective storms have been examined, to identify the environmental conditions supportive of strong updrafts and downdrafts. It is found that a combination of pseudoadiabatic CAPE [expressed in m s^{-1} via (2 CAPE)$^{0.5}$], bulk tropospheric wind shear, the temperature at cloud base, and LFC height account for a substantial amount

[3] Herein, we take the parcel with the largest DCAPE, regardless of its level of origin.

[4] However, this does *not* imply that a reversible adiabat is a better description of deep convective updrafts than is a pseudoadiabat (cf. Cohen and Frank 1989).

TABLE 7. As in Table 2, but using $(2\ \mathrm{RCAPE})^{0.5}$ to predict WMAX.

		$b_0 \ldots b_n$						
n	(y intercept)	−1.036	−30.222	−42.895	−33.622	−27.677	−26.763	−16.216
1	$\sqrt{(2\mathrm{RCAPE})}$ (m s^{-1})	0.525	0.742	0.717	0.904	1.025	1.024	0.952
2	VMAG (m s^{-1})		2.432	2.432	2.432	2.432	2.432	2.432
3	LFC (km)			10.955	10.523	10.243	12.071	12.240
4	ZMAXB (km)				−2.500	−2.345	−2.345	−2.111
5	ZMAXV (km)					−1.764	−1.764	−1.527
6	LCL (km)						−3.657	−6.006
7	T_{LCL} (°C)							−0.511
	r^2	0.40	0.56	0.65	0.70	0.72	0.73	0.74

(67%) of the interexperiment variance in storm updraft intensity. Alternatively, $(2\ \mathrm{RCAPE})^{0.5}$, VMAG, and LFC height account for 65% of the WMAX variance. Some environments (e.g., those that are ''CAPE starved'') fail to produce persistent storms, unless other conditions are especially favorable. Updrafts are wider in high-CAPE, high-shear environments, especially when the LFC is raised within reasonable bounds. In persistent storms, anticipation of downdraft strength is complicated by its microphysical properties, but the bulk wind shear, environmental temperature, and LFC height are the three environmental properties most closely related to peak downdraft velocity.

The environmental relative humidity, not studied herein, must also be considered when describing storm morphology (e.g., McCaul and Cohen 2004; Bunkers et al. 2006). McCaul and Cohen (2004) demonstrated that updrafts become weaker as the relative humidity above the LFC decreases. Further sensitivity studies involving model turbulence parameterizations are required to better evaluate these findings. Also, the influence of microphysical parameterizations must be recognized. Cohen and McCaul (2006) and van den Heever and Cotton (2004) have shown that by changing hydrometeor sizes and distributions, storm precipitation characteristics can vary considerably. In this study, we have kept the parameters that determine the size distributions of each hydrometeor species constant, to minimize the effects of such variations on the results. It is possible that these two factors, hydrometeor distributions and the environmental relative humidity, could contribute to additional variability in the regression analyses, especially for the downdraft.

While providing valuable insight into the general evolution of our simulated convective storms, the linear regression approach used herein does have some limitations. It should be noted that our seven environmental parameters do not predict any storm–environment relationship perfectly. Nonlinear storm dynamics, which cannot be fully characterized from linear relationships with ambient environmental conditions, work to reduce predictability of storm behavior. The pressure perturbations induced by interaction of the updraft with the ambient shear can impact storm rotation and strength, inflow and outflow trajectories, and overall storm evolution. In addition, the scatter of points in Fig. 3 hints at the possibility that nonlinearities might be worth considering in the regressions. Also, there may be other compound parameters that can be derived from ours that would improve the regressions somewhat (e.g., as with RCAPE versus PCAPE, discussed above).

The results are also limited to the envelope of environmental profiles possible in the COMPASS study. For example, it is not advisable to use these equations to ''forecast'' storm properties for simulations with CAPE much greater than 3200 J kg^{-1}, or with an LFC much greater than 1.6 km, etc. Nor are our regression equations intended to serve straightforwardly as predictors of ''real-world'' observed storm properties. Instead, this work only serves to organize and identify key features of the environmental sounding that influence storm updraft and downdraft strength and variability, and to help interpret the strength of those relationships.

The COMPASS simulation set continues to present an array of future research opportunities. The current work is being expanded to consider additional storm characteristics, such as the production of precipitation, storm rotation, and properties of the storm-generated cold pool. Sensitivities to microphysical parameters and to environmental relative humidity, discussed above, continue to be explored. The general trends in the results should also be compared against observational databases or climatologies of convective storms. More detailed exploration of the dynamics of storms is also possible using trajectory or pressure perturbation analyses.

Acknowledgments. Support for this research was provided by Grant 745245 from the National Oceanic and Atmospheric Administration, to Dr. Kevin Knupp

at the University of Alabama in Huntsville (UAH). The COMPASS study originated under Grant ATM-0126408 from the National Science Foundation under the supervision of Dr. Stephan Nelson. The COMPASS numerical simulations were conducted on the Matrix Linux cluster at UAH. We acknowledge programming support from Jayanthi Srikishen of USRA in Huntsville, and computer system support from Scott Podgorny, UAH, throughout this project. For additional information on the COMPASS study, see our Web site (http://space.hsv.usra.edu/COMPASS). The three anonymous reviewers are thanked for their thoughtful comments.

REFERENCES

Adlerman, E. J., and K. K. Droegemeier, 2005: The dependence of numerically simulated cyclic mesocyclogenesis upon environmental vertical wind shear. *Mon. Wea. Rev.,* **133,** 3595–3623.

Beebe, R. G., 1955: Types of airmasses in which tornadoes occur. *Bull. Amer. Meteor. Soc.,* **36,** 349–350.

Brooks, H. E., and J. P. Craven, 2002: Database of proximity soundings for significant severe thunderstorms, 1957–1993. Preprints, *21st Conf. on Severe Local Storms,* San Antonio, TX, Amer. Meteor. Soc., 639–642.

Bunkers, M. J., J. S. Johnson, L. J. Czepyha, J. M. Grzywacz, B. A. Klimowski, and M. R. Hjelmfelt, 2006: An observational examination of long-lived supercells. Part II: Environmental conditions and forecasting. *Wea. Forecasting,* **21,** 689–714.

Byers, H. R., and R. R. Braham, 1949: *The Thunderstorm*. U.S. Government Printing Office, 287 pp.

Cohen, C., and W. M. Frank, 1989: A numerical study of lapse-rate adjustments in the tropical atmosphere. *Mon. Wea. Rev.,* **117,** 1891–1905.

——, and E. W. McCaul Jr., 2006: The sensitivity of simulated convective storms to variations in prescribed single-moment microphysics parameters that describe particle distributions, sizes, and numbers. *Mon. Wea. Rev.,* **134,** 2547–2565.

Davies-Jones, R. P., 2002: Linear and nonlinear propagation of supercell storms. *J. Atmos. Sci.,* **59,** 3178–3205.

Droegemeier, K. K., and R. B. Wilhelmson, 1985: Three-dimensional numerical modeling of convection produced by interacting thunderstorm outflows. Part I: Control simulation and low-level moisture variations. *J. Atmos. Sci.,* **42,** 2381–2403.

Dutton, J. A., 1976: *Dynamics of Atmospheric Motion*. Dover Publications, Inc., 617 pp.

Emanuel, K. A., 1994: *Atmospheric Convection*. Oxford University Press, 580 pp.

Evans, J. S., and C. A. Doswell III, 2001: Examination of derecho environments using proximity soundings. *Wea. Forecasting,* **16,** 329–342.

Fawbush, E. J., and R. C. Miller, 1954: The types of air masses in which American tornadoes form. *Bull. Amer. Meteor. Soc.,* **35,** 154–165.

Fujita, T. T., 1981: Tornadoes and downbursts in the context of generalized planetary scales. *J. Atmos. Sci.,* **38,** 1511–1534.

Gilmore, M., and L. J. Wicker, 1998: The influence of midtropospheric dryness on supercell morphology and evolution. *Mon. Wea. Rev.,* **126,** 943–958.

Kirkpatrick, C., E. W. McCaul Jr., and C. Cohen, 2006: The influence of eight basic environmental parameters on the low-level rotation characteristics of simulated convective storms. Preprints, *23rd Conf. on Severe Local Storms.,* St. Louis, MO, Amer. Meteor. Soc., 16.3. [Available online at http://ams.confex.com/ams/pdfpapers/114923.pdf.]

——, ——, and ——, 2007: The motion of simulated convective storms as a function of basic environmental parameters. *Mon. Wea. Rev.,* **135,** 3033–3051.

Klemp, J. B., and R. B. Wilhelmson, 1978: The simulation of three-dimensional convective storm dynamics. *J. Atmos. Sci.,* **35,** 1070–1096.

Knupp, K. R., 1987: Downdrafts within High Plains cumulonimbi. Part I: General kinematic structure. *J. Atmos. Sci.,* **44,** 987–1008.

——, 1988: Downdrafts within high plains cumulonimbi. Part II: Dynamics and thermodynamics. *J. Atmos. Sci.,* **45,** 3965–3982.

Kuchera, E. L., and M. D. Parker, 2006: Severe convective wind environments. *Wea. Forecasting,* **21,** 595–612.

Lemon, L. R., and C. A. Doswell III, 1979: Severe thunderstorm evolution and mesocyclone structure as related to tornadogenesis. *Mon. Wea. Rev.,* **107,** 1184–1197.

Marwitz, J. D., 1972: The structure and motion of severe hailstorms. Part I: Supercell storms. *J. Appl. Meteor.,* **11,** 166–179.

McCaul, E. W., Jr., and M. L. Weisman, 1996: Simulations of shallow supercell storms in landfalling hurricane environments. *Mon. Wea. Rev.,* **124,** 408–429.

——, and ——, 2001: The sensitivity of simulated supercell structure and intensity to variations in the shapes of environmental buoyancy and shear profiles. *Mon. Wea. Rev.,* **129,** 664–687.

——, and C. Cohen, 2002: The impact on simulated storm structure and intensity of variations in the mixed layer and moist layer depths. *Mon. Wea. Rev.,* **130,** 1722–1748.

——, and ——, 2004: The initiation, longevity and morphology of simulated convective storms as a function of free tropospheric relative humidity. Preprints, *22nd Conf. on Severe Local Storms,* Hyannis, MA, Amer. Meteor. Soc., CD-ROM, 8A.5. [Available online at http://ams.confex.com/ams/pdfpapers/81251.pdf.]

——, ——, and C. Kirkpatrick, 2005: The sensitivity of simulated storm structure, intensity, and precipitation efficiency to environmental temperature. *Mon. Wea. Rev.,* **133,** 3015–3037.

Newton, C. W., and J. C. Fankhauser, 1975: Movement and propagation of multicellular convective storms. *Pure Appl. Geophys.,* **113,** 747–764.

Pielke, R. A., and Coauthors, 1992: A comprehensive meteorological modeling system—RAMS. *Meteor. Atmos. Phys.,* **9,** 69–91.

Rasmussen, E. N., and D. O. Blanchard, 1998: A baseline climatology of sounding-derived supercell and tornado forecasting parameters. *Wea. Forecasting,* **13,** 1148–1164.

——, and J. M. Straka, 1998: Variations in supercell morphology. Part I: Observations of the role of upper-level storm-relative flow. *Mon. Wea. Rev.,* **126,** 2406–2421.

Rotunno, R., J. B. Klemp, and M. L. Weisman, 1988: A theory for strong, long-lived squall lines. *J. Atmos. Sci.,* **45,** 463–485.

Srivastava, R. C., 1987: A model of intense downdrafts driven by the melting and evaporation of precipitation. *J. Atmos. Sci.,* **44,** 1752–1774.

Thompson, R. L., R. Edwards, J. A. Hart, K. L. Elmore, and P. Markowski, 2003: Close proximity soundings within supercell environments obtained from the Rapid Update Cycle. *Wea. Forecasting,* **18,** 1243–1261.

Tripoli, G. J., and W. R. Cotton, 1982: The Colorado State University three-dimensional cloud/mesoscale model–1982.

Part I: General theoretical framework and sensitivity experiments. *J. Rech. Atmos.,* **16,** 185–219.

van den Heever, S., and W. R. Cotton, 2004: The impact of hail size on simulated supercell storms. *J. Atmos. Sci.,* **61,** 1596–1609.

Wakimoto, R. M., 2001: Convectively driven high wind events. *Severe Convective Storms, Meteor. Monogr.,* No. 27, Amer. Meteor. Soc., 570 pp.

Weisman, M. L., 1993: The genesis of severe, long-lived bow echoes. *J. Atmos. Sci.,* **50,** 645–670.

——, and J. B. Klemp, 1982: The dependence of numerically simulated convective storms on vertical wind shear and buoyancy. *Mon. Wea. Rev.,* **110,** 504–520.

——, and ——, 1984: The structure and classification of numerically simulated convective storms in directionally varying shears. *Mon. Wea. Rev.,* **112,** 2479–2498.

Wicker, L. J., and L. Cantrell, 1996: The role of vertical buoyancy distributions in miniature supercells. Preprints, *18th Conf. on Severe Local Storms,* San Francisco, CA, Amer. Meteor. Soc., 225–229.